



4<sup>th</sup> IASPEI / IAEE International Symposium:

## Effects of Surface Geology on Seismic Motion

August 23–26, 2011 • University of California Santa Barbara

### GEOTECHNICAL DOWNHOLE ARRAYS RECENTLY DEPLOYED IN ISTANBUL

**Aslı Kurtuluş**  
Boğaziçi University  
Istanbul, 34684  
Turkey

**Atila Ansal**  
Boğaziçi University  
Istanbul, 34684  
Turkey

**Erdal Şafak**  
Boğaziçi University  
Istanbul, 34684  
Turkey

#### ABSTRACT

Recently, three geotechnical downhole arrays are deployed in the west European side of Istanbul, Turkey with efforts of Kandilli Observatory and Earthquake Research Institute (KOERI). Existing high seismic activity of the region increases the scientific importance of these downhole arrays. Each array is composed of one accelerometer on the ground surface and three or four borehole accelerometers at various depths along the soil profile with the deepest sensor located at the engineering bedrock level ( $V_s > 750$  m/s). The arrays also provide reference bedrock motion for Rapid Response Network composed of 55 surface instruments operated by KOERI in the west European side of city. Preliminary analysis of the weak ground motion data provides evidence for significant site amplification by the surface layers and indicates that  $V_{S30}$  alone is not a sufficient indicator of site amplification potential. Apart from conventional methods recorded borehole data is also analyzed using a technique referred as seismic interferometry. This technique is based on the correlation of waves recorded by different receivers and allows for extraction of soil properties from the recorded time-histories. Analysis of weak motion borehole records from Istanbul arrays shows that wave velocity profiles obtained using seismic interferometry are in agreement with those determined from in-hole geophysical seismic wave velocity measurements. Moreover, it is possible to quantify intrinsic attenuation of the encountered soil layers.

#### INTRODUCTION

Estimation of site specific ground motion characteristics has been a crucial issue in the assessment of the vulnerability of the existing structures, for retrofit and rehabilitation alternatives as well as in the design of new structures. The scientific aspects contain significant degree of uncertainties and reliable solution of this problem requires development of realistically comprehensive numerical and analytical models that rely on large amount of field evidence. Downhole seismic arrays, which are deployed in seismically active areas to record ground motion during earthquakes, are one of the ways to collect field evidence for soil response. The information provided by these arrays is considered very valuable for verification, calibration and development of predictive tools that are used in earthquake engineering. Acceleration records obtained during recent earthquakes have demonstrated that geological and geotechnical site conditions such as soil stratification, depth of ground water table, and properties of soil layers could have significant influence on strong motion characteristics on the ground surface (Beresnev et al. 1998, Trifunac and Todorovska 1998, Fukushima et al. 2000). The differences in the soil profiles even within relatively short distances and observations in previous earthquakes indicate that site conditions are important. Recently, Kandilli Observatory and Earthquake Research Institute (KOERI) has been implementing a strong motion network composed of vertical and horizontal arrays within the city of Istanbul, Turkey. The existing high seismic activity of the region increases the scientific importance of these arrays.

#### DOWNHOLE ARRAYS OF ISTANBUL

At this stage, three downhole arrays composed of four or three borehole accelerometers and one surface accelerometer are deployed in the western European Side of Istanbul. The support for the first array is granted by a joint effort from Istanbul Metropolitan Municipality (IMM) and Geo Forschungs Zentrum Potsdam (GFZ). Support for the two other arrays comes from a research project funded by The Scientific and Technological Research Council of Turkey (TÜBİTAK) and Boğaziçi University. The sites are

determined after careful evaluation of all data collected from an extensive site investigation study conducted as part of a large scale microzonation project of IMM for western European Side of Istanbul which was carried out with technical guidance from KOERI. Approximately 2900 boreholes (14 of them deeper than 100m) were drilled within an area of about 182 km<sup>2</sup> to investigate local soil conditions. Various field and laboratory tests were conducted to determine the geotechnical and geophysical properties of soil layers (OYO 2007). All this data is compiled and evaluated to decide on appropriate locations for installation of arrays. Depth of bedrock, properties of soil profile, seismic vulnerability of the area and the overall security of the site have been the main concerns while selecting the most appropriate sites for installation. Once selected, local site conditions at each downhole array location are investigated in more detail by means of Standard Penetration Tests (SPT), in-hole seismic measurements (PS Logging Tests), and a number of laboratory tests conducted on soil samples collected from the field. The locations of recently deployed Istanbul geotechnical downhole arrays are shown in Fig.1. Details about instrumentation and site conditions at each station are given below. All boreholes that are instrumented have been ‘rotary-mud’ drilled, PVC cased and grout injected prior to installation of three-component downhole force-balance accelerometers (FBA).

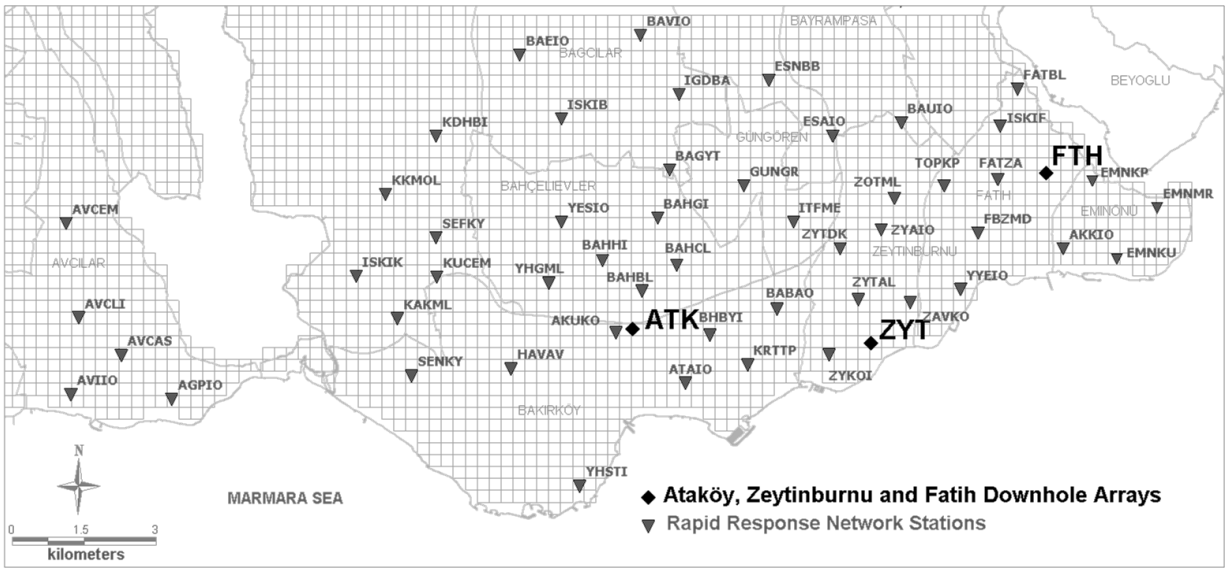


Fig. 1. Istanbul Strong Motion Network (250mx250m grids for Istanbul Microzonation Project are shown in the background)

### Ataköy Array

Ataköy downhole array (ATK) is located close to the Atatürk International Airport and represents a stiff-soil/rock site. Geologically, the site can be characterized with a Miocene age unit known as Güngören formation underlain by Eocene age Ceylan Formation. Güngören formation is mostly associated with hard clay and sand layers but also includes limestone. Ceylan formation consists of sandstone and claystone and represents bedrock layer with an approximate depth of 100-150m at this part of the city. Geotechnical site investigations carried out at the array location revealed that the soil profile is composed of alternating hard sandy clay and dense to very dense clayey sand layers down to 110m while sandstone is encountered below this depth. Between the depths of 5m-34m there is a layer of highly weathered limestone with clay interlayers. These clay interlayers as well as the overlying sandy clay layer are classified as CL (PI=16-26, FC=52-56%). Below the depth of 35m, clay layers are more plastic (PI= 51-56) and have higher fines content. Dense sand layers down to the depth of sandstone layer are classified as SM and comprised of 16-34% fines with nonplastic nature. Average shear wave velocity profile inferred from PS Logging tests and soil layering obtained from geotechnical investigations are given in Fig. 2a. According to the profile presented in Fig. 2a, the equivalent shear wave velocity for the top 30m of the soil profile ( $V_{S30}$ ) at the site is approximately 278m/s.

ATK is composed of four triaxial accelerometers that are installed at depths of 25, 50, 70 and 140m and one triaxial accelerometer on the ground surface. Schematic illustration of the instrumentation at this station is shown in Fig. 3. Sensors at depths of 25m, 50m and 70m are Kinometrics SBEPI, while the deepest sensor is Kinometrics FBA ES-DH (with in-built compass). All four of the borehole sensors are connected to a 12-ch Kinometrics K2 Digital Recorder. A second digital recorder, a 4-ch Kinometrics K2 with internal three-component accelerometer, records the motion on the ground surface. Common triggering and GPS timing between the borehole sensors and the sensor at the ground surface allows for synchronized recording. Threshold-triggered data collected at a rate of 200 samples per second is periodically retrieved via ADSL connection. Among the borehole sensors only the deepest borehole sensor has a built-in compass for accurate orientation. The orientations of other three borehole sensors are determined through analysis of recorded acceleration-time histories (Kurtuluş et al. 2008).

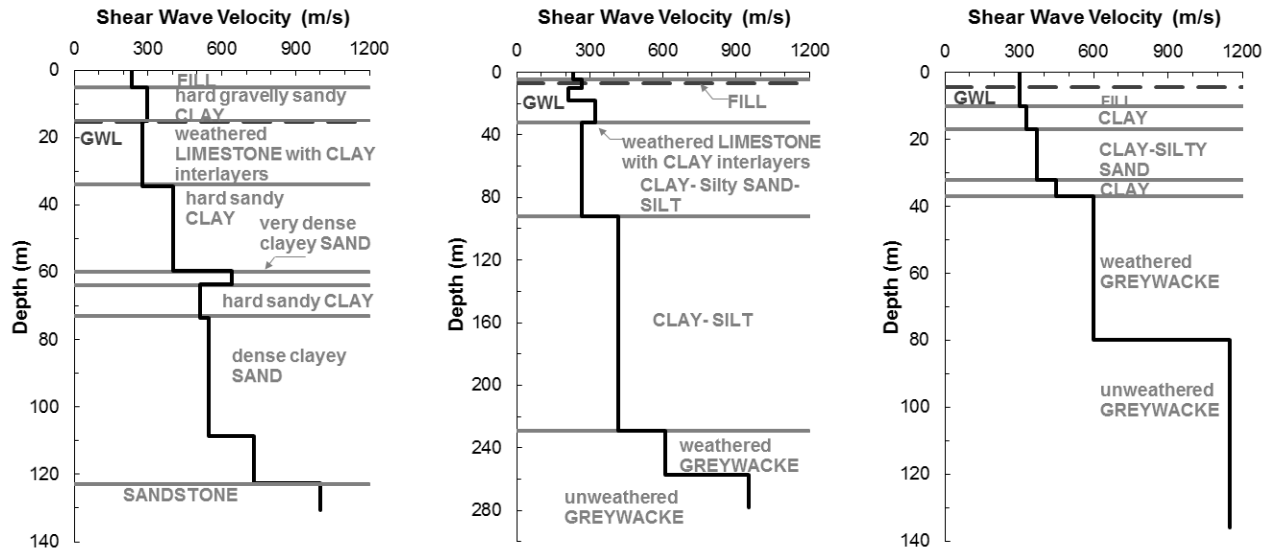


Fig. 2. Shear wave velocity profiles inferred from PS-Logging tests at a) ATK, b) ZYT, and c) FTH downhole array sites.

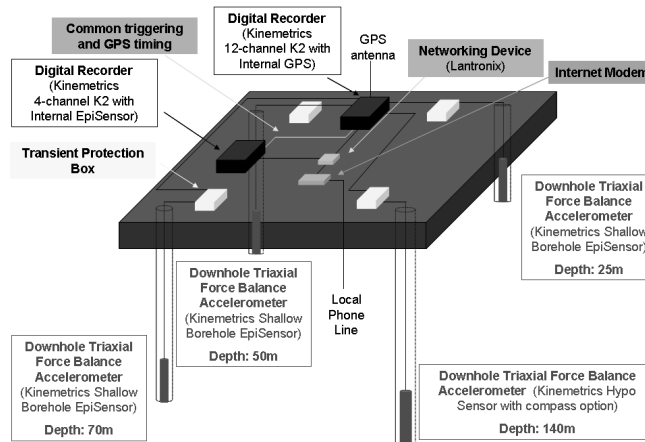


Fig. 3. Schematic illustration of the instrumentation at ATK downhole array site.

### Zeytinburnu Array

Zeytinburnu downhole array (ZYT) is located close to the shoreline at south west of the city and represents a relatively soft-soil/rock site. According to recently conducted seismic damage scenario studies, Zeytinburnu district represents one of the most vulnerable areas in the city (Ansal et al. 2010). Geologically, the site can be characterized by Miocene age units known as Bakırköy and Güngören formations. Bakırköy formation overlies Güngören formation and is associated with a 5 to 10m thick limestone layer containing thin layers of clay. Underlying these is the Paleozoic age Trakya formation composed of sandstone and shale (greywacke) which represents the bedrock layer. Trakya formation is encountered at a depth of about 200-250m at this part of the city. Geotechnical site investigations carried out at Zeytinburnu downhole array location revealed that the soil profile is composed of alternating clay and silt layers down to 230m while greywacke is encountered below this depth. Between the depths of 5m-32m there is a layer of weathered limestone with clay interlayers. Clay layers alternate between CL (PI= 13-22) and CH (PI=37-67) while silt layers are classified as MH (PI=22-49). Fines content of CL, CH and ML materials are typically very high (FC=72-100). Thin layers of silty sand (SM) are encountered occasionally between the alternating clay and silt layers. Average shear wave velocity profile inferred from PS Logging tests and soil layering obtained from geotechnical investigations are given in Fig. 2b. According to the profile presented in Fig. 2b,  $V_{S30}$  at the site is equal to 263m/s. ZYT is composed of three triaxial accelerometers that are installed at depths of 30, 57, and 288m and one triaxial accelerometer on the ground surface, using a similar field set-up to that shown in Fig. 3, but with more up-to-date instrumentation. All boreholes are instrumented with Kinematics FBA ES-DH (with in-built compass) while an external three-component accelerometer (Kinematics EpiSensor) is installed on the ground surface. All sensors are oriented to exact North. Sensors are connected to a 12-ch Kinematics Rock Digital Recorder which allows for threshold-triggered data collected at 200 samples per second to be automatically sent to an ftp website of KOERI via ADSL connection.

## Fatih Array

Fatih downhole array (FTH) is located on a hill adjacent to a seismically monitored historical mosque within the old city and represents a stiff-soil/rock site. Historically the site has always been an important location for religious structures (dating as early as 550 BC) most of which had been significantly damaged during the past major earthquakes. Ground accelerations as high as 0.2g have been recorded at this site during the  $M_w = 7.4$ , 1999 Kocaeli Earthquake which was located about 100km away from Istanbul. Geologically, the site has similar features as ZYT site which can be characterized by the Miocene age units known as Bakırköy and Güngören formations underlain by the Paleozoic age Trakya formation representing the bedrock layer. Trakya formation is encountered at a depth of approximately 60-80m at this part of the city. Geotechnical site investigations carried out at this location revealed that the soil profile is composed of alternating clay, silty sand layers up to 40m while greywacke is encountered below this depth. It was observed that the top 40m of greywacke is considerably weathered and the intact material is located at a depth of about 80m. Clay layers are mostly classified as CH (PI=32-59), occasionally as CL (PI=14-24) at shallower depths (<10m). Fines content of these materials are variable (FC= 63-93%). Silty sand (SM) layers with FC=14-43% are encountered between the clay layers at the depths of 17 to 32m. Average shear wave velocity profile inferred from PS Logging tests and soil layering obtained from geotechnical investigations are given in Fig.2c. According to the profile presented in Fig. 2c,  $V_{S30}$  at this site is equal to 335m/s. FTH is composed of four triaxial accelerometers that are installed at depths of 23m, 60m, 136m and on the ground surface. Instrumentation and field set-up at this site is identical to that at ZYT array. Given the fact that Fatih Mosque is also instrumented and monitored by KOERI, the site is expected to provide valuable data not only for free-field soil response but also for soil-structure interaction related studies.

## RAPID RESPONSE NETWORK

Istanbul Rapid Response Network (IRRN), operated by KOERI, is composed of 100 strong motion stations distributed within the city of Istanbul. The network consists of strong-motion instruments (Güralp CMG-5T) located at grade level in small- to medium-sized buildings. Full-recorded waveforms at each station can be retrieved using GSM and GPRS modems subsequent to an earthquake (Erdik et al. 2003). Out of 100 rapid response network strong motion stations, 55 stations are located in the European side of Istanbul (Fig.1). As mentioned before a comprehensive site investigation study involving 2900 geotechnical borings was conducted for this area (OYO 2007). The data included mostly Standard Penetration Test (SPT), seismic reflection, seismic refraction measurements and some Cone Penetration Test (CPT) and PS-Logging measurements as well as a number of laboratory test results from disturbed soil samples. The information compiled is used to obtain a representative soil profile at each IRRN station. Profiles for some of the stations are illustrated in Fig. 4. Measurements performed at borings conducted in the near vicinity (<200m) of the stations are taken into account in determining these profiles. Depths of engineering bedrock are typically estimated based on the 3D engineering bedrock model that was prepared during the Istanbul Microzonation Project (OYO 2007). Variations of  $V_{S30}$  and depth to bedrock formation at IRRN stations are shown in Fig. 5. As can be observed from Fig.5, all station sites have comparable  $V_{S30}$  values while depths of bedrocks are quite variable.

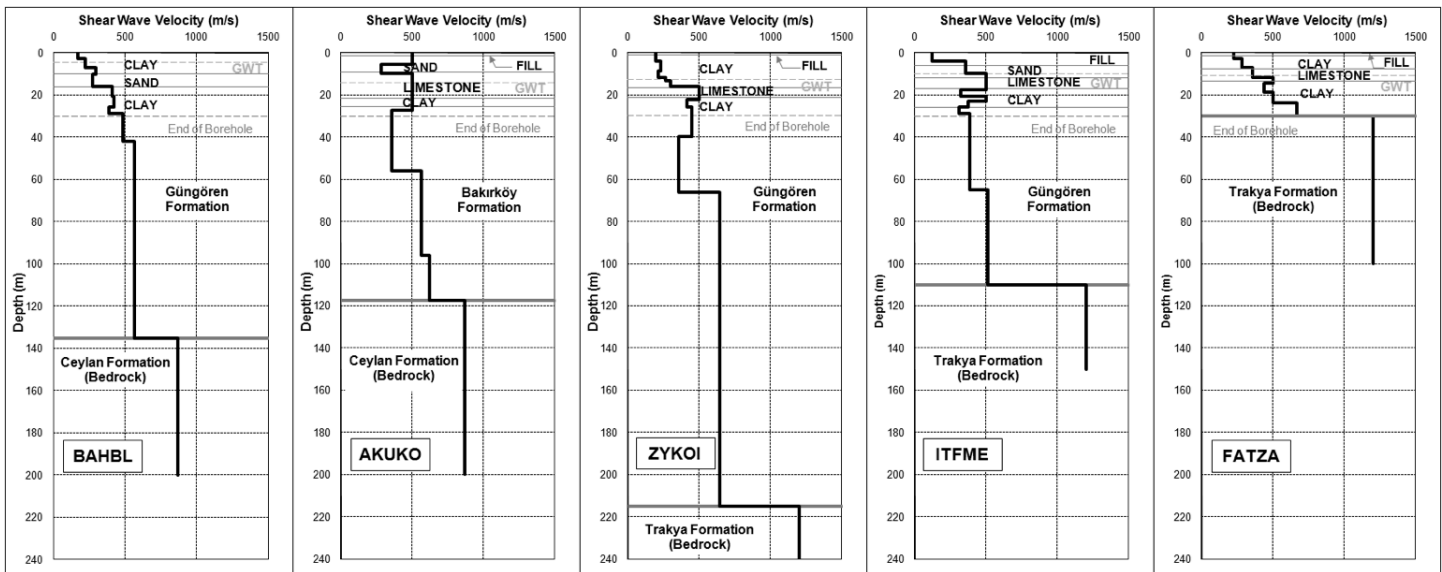


Fig. 4. Representative shear wave velocity profiles for some of the IRRN station sites (from geophysical tests conducted for Istanbul Microzonation Project).

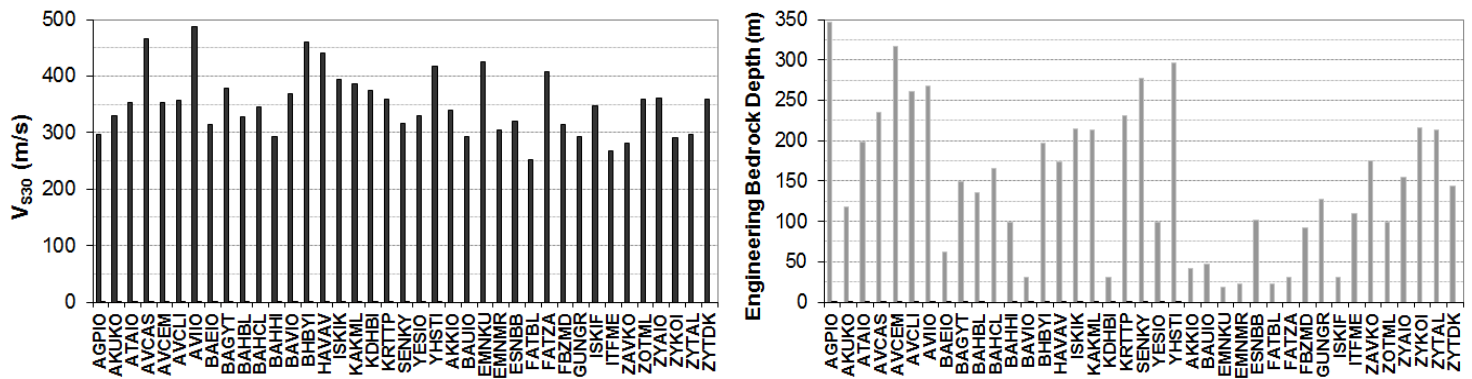


Fig. 5. Variation of a)  $V_{S30}$ , and b) depth of engineering bedrock at IRRN station sites.

## RECORDED MOTIONS

All three downhole arrays are relatively new, therefore only a number of small magnitude earthquakes have been recorded so far. Among the three, ATK has been recording for the longest period of time (since 2007). The other two arrays are more recently deployed and have been in operation for less than a year. A list of most significant events ( $M > 4.0$ ,  $R < 200$  km) recorded at these stations is given in Table 1. Maximum ground accelerations recorded at the sites so far does not exceed 0.01 g. Among the earthquakes listed in Table 1, 12.03.2008 Çınarcık, 03.10.2010 Marmara and 19.05.2011 Kütahya events have also been recorded by IRRN stations. On the European side of city, 29 stations recorded the Çınarcık event while only 22 stations were able to record the Marmara and Kütahya events. Location of epicenters of these events with respect to the accelerometer arrays are shown in Fig. 6. All are shallow events (depth of ~11 km) generated by different segments of EW strike-slip North Anatolian Fault (NAF). As can be observed from Fig. 6 and Table 1, epicentral distances of the two earlier events are quiet similar with almost perpendicular azimuths while the latest event occurred at a much larger distance (~200 km) yet in similar direction with the 12.03.2008 Çınarcık event.

Table 1. List of  $M_L > 4$  local events recorded by downhole arrays in Istanbul

Eq. No	Date/Local Time	Local Name	Lat. °	Long. °	Depth (km)	$M_L$	Station	Distance (km)	$PGA_{surface}(g)$
1	12/03/2008/18:53:39	Çınarcık	40.620	29.004	11.2	4.8	ATK	43.4	0.008
2	05/10/2008/09:04:05	-	40.650	29.017	8.5	4.1	ATK	41.6	0.002
3	24/01/2009 15:58:38	-	40.803	27.785	11.2	4.2	ATK	91.7	0.001
4	27/04/2009 19:03:06	-	40.759	27.543	18.2	4.1	ATK	115.5	0.003
5	01/08/2009 16:42:38	-	40.366	28.274	9.1	4.1	ATK	85.3	0.001
6	08/08/2009 13:52:38	-	40.328	27.411	15.6	4.4	ATK	141.8	0.001
7	03/10/2010 20:49:02	Marmara	40.846	28.110	11.2	4.4	ATK, ZYT	64.2, 68.8, 73.2	0.008, 0.008
8	19/05/2011 23:15:23	Kütahya	39.152	29.088	7.6	5.9	ATK, ZYT, FTH	205.5, 204.8, 208.2	0.005, 0.006, 0.011

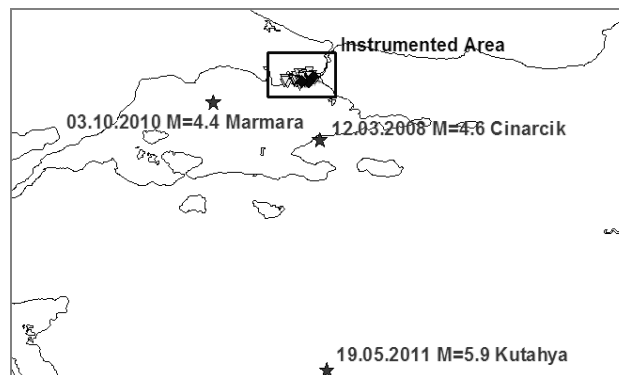


Fig. 6. Epicenters of 12/03/2008  $M=4.8$  Çınarcık, 03/10/2010  $M=4.4$  Marmara and 19/05/11  $M=5.9$  Kütahya events

Response spectra of downhole records from the three events are shown in Fig. 7. The effect of distance can be readily seen by comparing response at Kütahya event with that observed during the two other events. Even if similar spectral accelerations are recorded and all at linear range, frequency response can be quite different depending on the distance and source effects. Also seen from Fig. 7, at each site records obtained from the two deepest sensors are similar to each other in terms of amplitude while evidence of amplification by the surface layers is observed on records obtained at shallower depths. However, an unexpected phenomenon appears at shallow depths at the ATK and ZYT sites such that the amplitude of accelerations recorded at depths of 25m and 30m, respectively, are similar to those recorded by the deepest sensors. In other words, deamplification of motion is observed at these depths. Other records obtained at the two sites also exhibit the same behavior. The existence of weathered limestone layer at this depth is somehow thought to be a reason for observing smaller amplitude accelerations, even though the average wave velocity profiles inferred from PS Logging tests do not give an indication of such behavior. Similar trend is not observed in FTH site where the soil profile does not include the 'limestone' layer. It is decided that this shallow layer, which exists at many locations within the old city, requires more investigation.

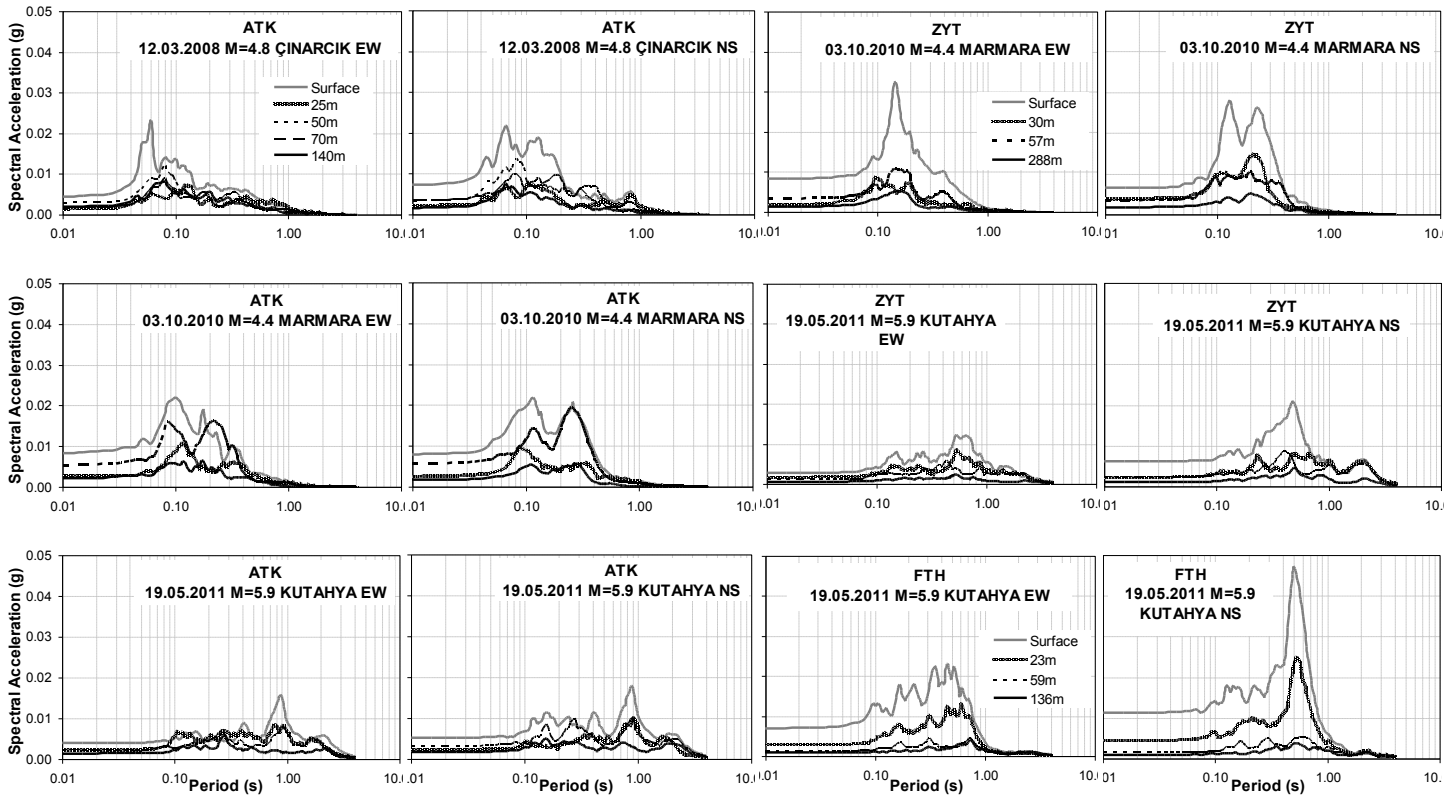


Fig. 7. Acceleration spectra of downhole records during the 12/03/2008 M=4.8 Çınarcık, 03/10/2010 M=4.4 Marmara and 19/05/11 M=5.9 Kütahya events

Average of surface/bedrock spectral ratio at each array site is shown in Fig. 8. As can be observed from Figs.7 and 8 amplification potential of FTH seems to be the greater than the others even though ZYT is a softer and deeper site. Observed spectral ratios show that the average amplification from bedrock to the surface of the soil reaches a factor of 4, 7 and 12 at periods of 0.9 s, 1.5 s and 0.5s at ATK, ZYT and FTH sites, respectively. At ATK and FTH sites, the values of predominant periods observed from amplification spectra seem to be in agreement with theoretical 1D fundamental periods of 1.1 and 0.6, respectively, that are calculated from the measured wave velocity profiles using the well-known  $V_s=4H/T_0$  relationship. However, calculated fundamental period suggests a longer period (2.7 s) for ZYT than that observed from the records obtained at this site. On the other hand, the observed higher amplification potential of FTH site is related to the similarity of the fundamental period of the site to that of the recorded event (~0.6s).

Recorded response at the IRRN stations during the same events are shown in Fig.9, NEHRP (2001) soil classes of station sites are also indicated. A significant variation is observed for all three events with average cov (coefficient of variation) in the range of 0.6 to 0.8. Variations of PGA and PSA (peak spectral acceleration) are further compared in Figs. 10 with respect to epicentral distance and NEHRP (2001) site classes. According to the information presented in Fig. 9, it is possible to say that for both ground shaking

parameters all three events generate similar range of values with Marmara event producing slightly higher ground shaking. Also seen from Fig. 10, the epicentral distances for the Çınarcık and Marmara events can be considered in the same range ( $<75\text{km}$ ) compared to Kütahya event occurring at distance slightly greater than  $200\text{km}$ . The effect of distance has introduced differences not in the recorded peak ground accelerations but rather in the frequency content of the response. Response spectra observed during the Kütahya event clearly shows a shift towards larger periods. Another observation is that spectra of motions recorded during the NS directional Çınarcık and Kütahya events exhibit a broader frequency band when compared to those observed during the EW directional Marmara event. Considering the EW mechanism of (NAF), the difference may be attributed to directivity/path effects.

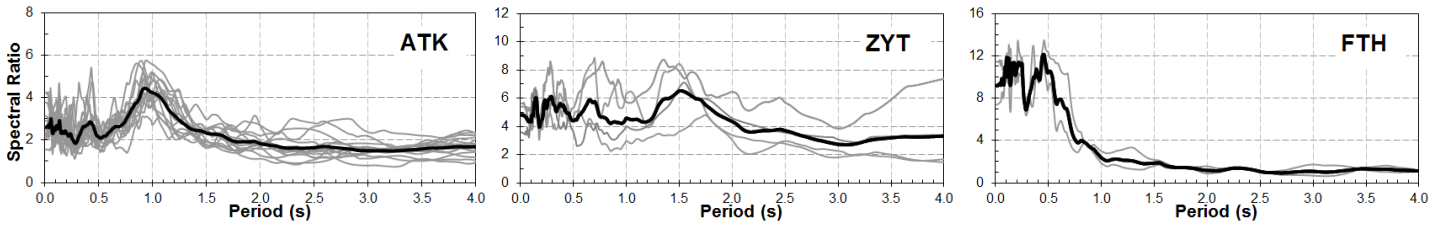


Fig. 8. Average site amplification (surface/bedrock) at ATK, ZYT, and FTH sites calculated from events  $4.0 < M < 4.7$  and  $40 \text{ km} < R < 200 \text{ km}$  (listed in Table 1)

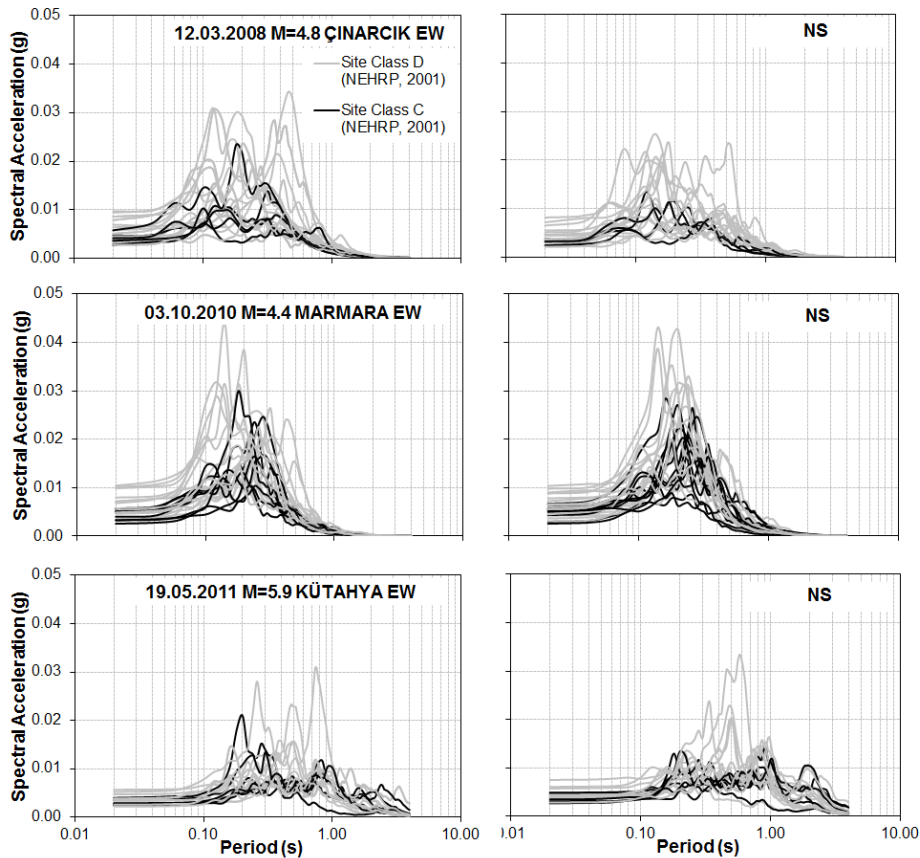


Fig. 9. Acceleration spectra recorded by IRRN stations in relation to NEHRP Site Class

On the other hand, the observed high scatter of the ground motions recorded during each event suggests that a significant part of the observed variation can be related to site effects. The variations of ground motion parameters with respect to NEHRP (2001) site classes show some indication of site effects (i.e. stations sites identified as Site C tend to have lower spectral response) but also demonstrate that  $V_{S30}$  alone is not a sufficient indicator for amplification potential, as observed from the significant scatter in the spectral response of stations located on Site D soils. As shown in Fig. 5, almost all strong motion stations have comparable  $V_{S30}$  values.

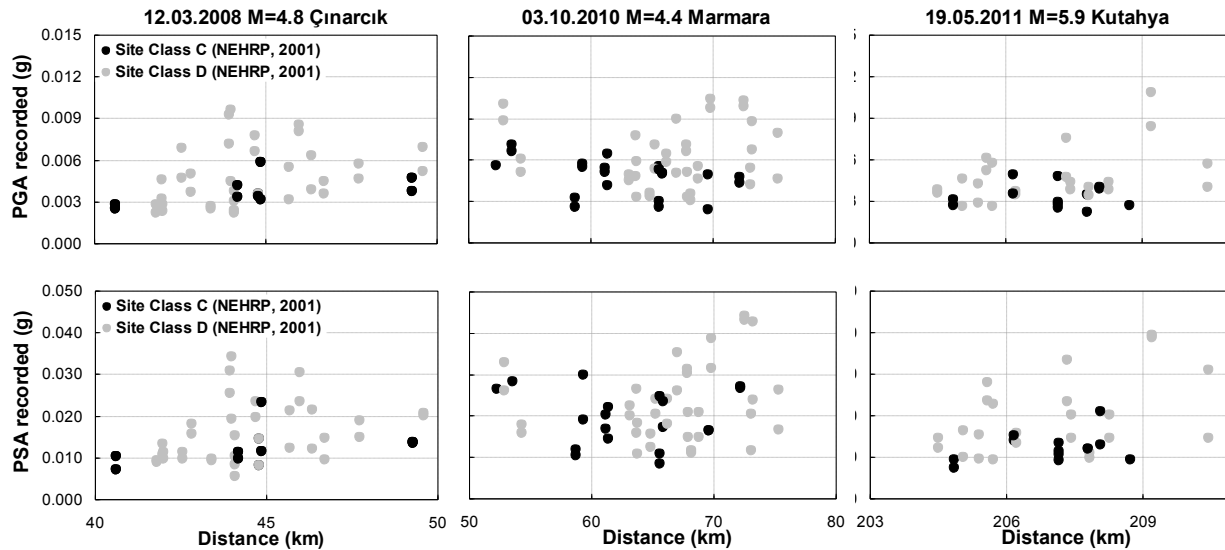


Fig. 10. Variations of PGA and PSA recorded by IRRN stations with epicentral distance and in relation to NEHRP (2001) Site Class (both EW and NS components are shown)

## RECORDED AND MODELED RESPONSE

An attempt is made to estimate site-specific ground motion parameters at IRRN stations by performing 1D response analysis using Shake91 (Idriss and Sun 1992) with the assumption that time histories recorded by the deepest accelerometers at ATK, ZYT and FTH downhole arrays can represent bedrock motions for these sites. A comparison of deepest accelerometer records obtained at the sites is shown in Fig. 11. As observed from Fig. 11, the recorded bedrock motions have differences in both frequency and amplitude response. The differences are less pronounced between the ZYT and FTH sites. One possible reason could be that the properties of the engineering bedrock with measured  $V_s$  in the range of 1000 m/s do not sufficiently represent the engineering bedrock. Another reason could be the differences in the geological formations at these locations. Bedrock model for the region suggests that FTH and ZYT sites are located on Trakya formation; geologically an older age formation than Ceylan formation that underlies ATK site.

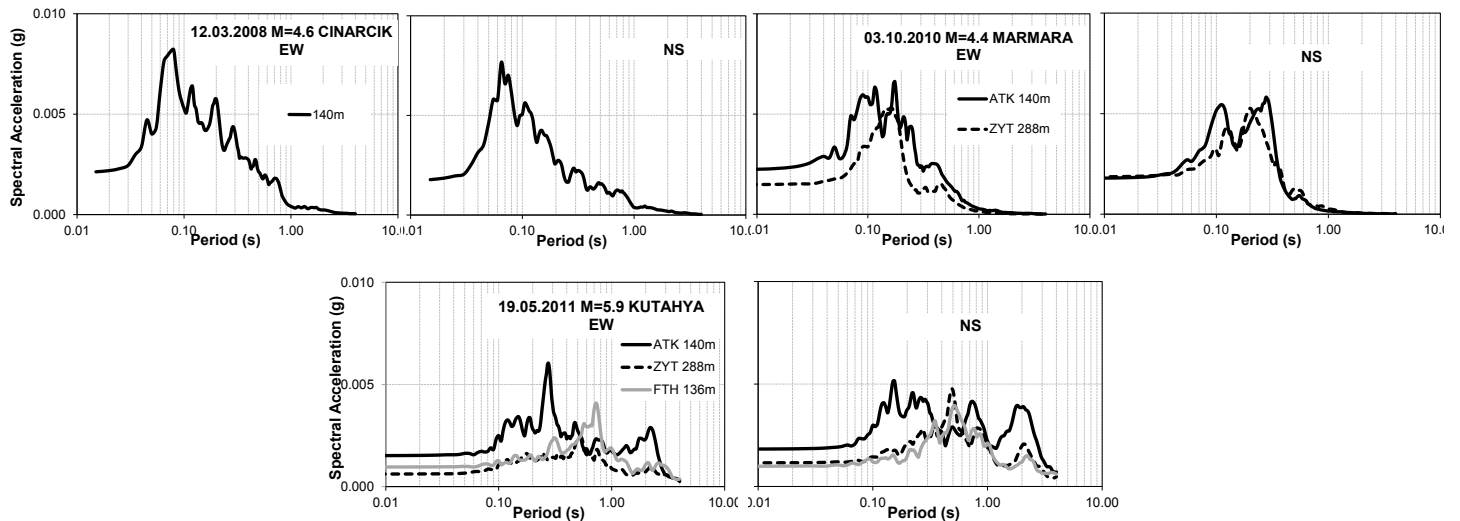


Fig. 11. Acceleration spectra of records obtained from the deepest downhole accelerometers at ATK, ZYT, and FTH sites

Site response modelling is carried out for 10 of the IRRN stations that recorded all three events. In the analysis, the bedrock acceleration time histories recorded at ATK, ZYT and FTH are used as input motions. A comparison of the recorded and modelled PGA and PSA values are shown in Fig. 12. In general, there is a certain agreement between the recorded and the calculated parameters (mean squared error < 0.2). However, as seen in the figure, calculated ground motion parameters are different from each



other depending on the input acceleration time history. ZYT seems to be providing the best-fitting bedrock motion. One reason could be the associated bedrock geology; another possible reason is the selection of ground motion parameter used in the comparisons. It may be necessary to investigate other ground motion characteristics to evaluate the most representative bedrock reference.

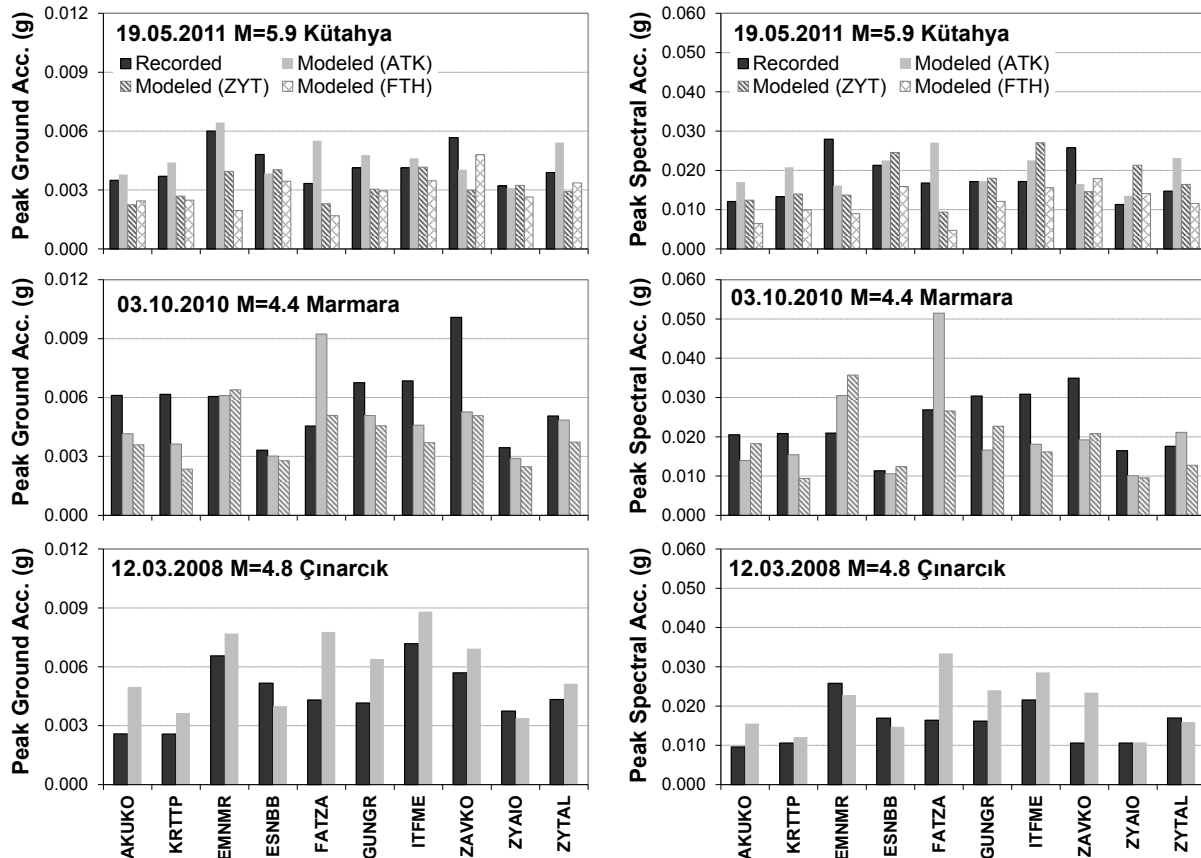


Fig. 12. Comparison of the recorded and modeled ground motion parameters at the 10 IRRN stations (logarithmic mean of the two horizontal components are considered)

#### APPLICATION OF SEISMIC INTERFEROMETRY TO DOWNHOLE RECORDS

Downhole records are also used to investigate for applicability of a technique referred as seismic interferometry. The technique is usually based on cross correlation of waves recorded at different receivers. Elgamel et al. (1995) applied cross-correlation to the Lotung array records and have been able to obtain soil response characteristics. Snieder and Safak (2006) used seismic interferometry by deconvolving waves instead of cross-correlating them and extracted the building response. Mehta et al. (2007) have applied the technique proposed by Snieder and Safak (2006) to Treasure Island array records to extract 1-D velocity profile of soil layers. Here, a similar approach is used by first applying deconvolution to waves recorded at different depths to separate the response of soil layers from the incoherent waveforms excited by an earthquake. In contrast to customary, waveforms are deconvolved using the surface recording (instead of motion recorded at the bedrock level) in order to obtain a simple downgoing wave as proposed by Snieder and Safak (2006). Once response of layers are isolated from interacting up and downgoing waves, wave travel times between the receivers are calculated to obtain wave propagation velocities. The two standard approach to calculate wave travel times between two recording points is to use the time differences between characteristics peaks or to determine the time lag where the cross-correlation of the waveforms has a maximum. However, these methods are acceptable for non-dispersive, non-attenuating media, where the waveforms do not change their shape as they travel. In fact, waves do change their shapes due to attenuation while travelling through soil layers. In other words, the phase shifts between the two records at different depths are caused by the combined effect of wave travel times plus the phase distortions due to damping. It is possible to eliminate the phase shifts introduced by damping on the calculated wave travel times by using the envelope functions of the waveforms. The travel times obtained from the envelope functions will be smaller; the difference representing the phase shift due to damping. The damping values corresponding to these phase shifts can be calculated and will constitute the intrinsic part of attenuation for the soil medium (Safak, 1995).

Acceleration-time histories recorded at ZYT site during the 19.05.2011 Kütahya event are used to demonstrate the applicability of this approach. Figure 13a shows the NS component of the raw records. The time- windowed accelerations showing the arrival of S waves are shown in Figure 13b. Deconvolution is applied to the signals shown in Figure 13b.

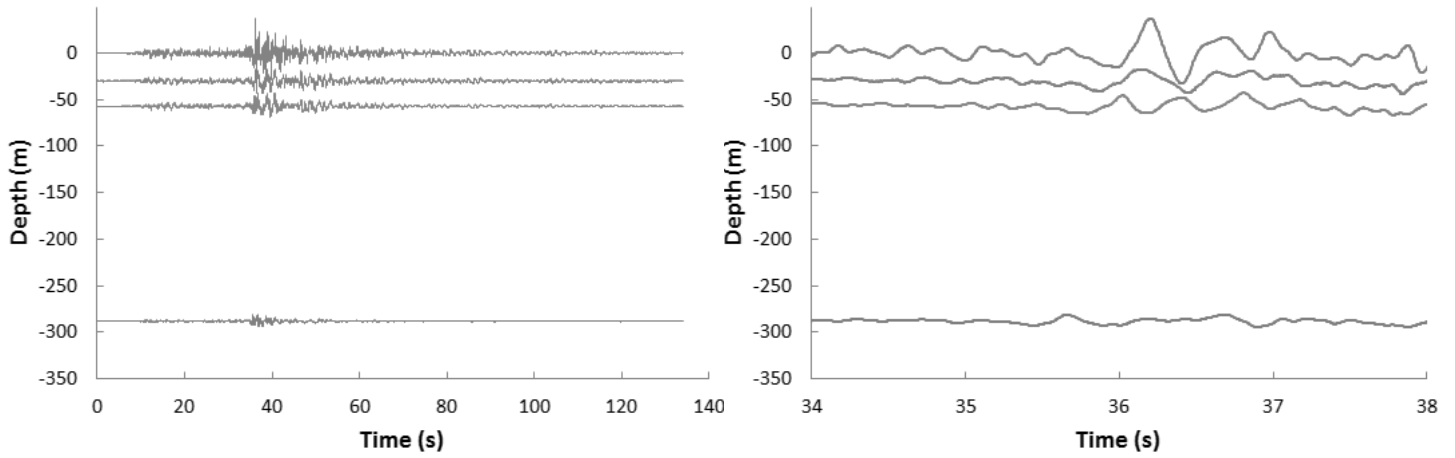


Fig. 13. NS component of 19.05.2011 Kütahya event recorded at ZYT site a) raw acceleration-time histories, and b) time-window showing S-wave arrival

In order to avoid instability, regularized deconvolution is performed using,

$$D(\omega) = A(\omega) * B(\omega) / (|B(\omega)|^2 + \epsilon) \quad (1)$$

where the asterix denotes complex conjugate and  $\epsilon$  is white-noise parameter added at the denominator to prevent instability (Snieder and Safak, 2006). Figure 14a shows the waveforms after deconvolving the waves at each depth with the waves at the surface using the S-wave window shown in Fig. 13b, while Figure 14b shows deconvolved waves after band-pass filtering around a narrow frequency band (1Hz-3Hz) centered at the predominant frequency (~2Hz) and increasing the sample rate of the waveforms to 1000sps in order to have sufficient accuracy for calculation of wave travel times. As seen from Fig. 14a and b, after deconvolution with the surface record, the acceleration records at depth become a simple downgoing wave.

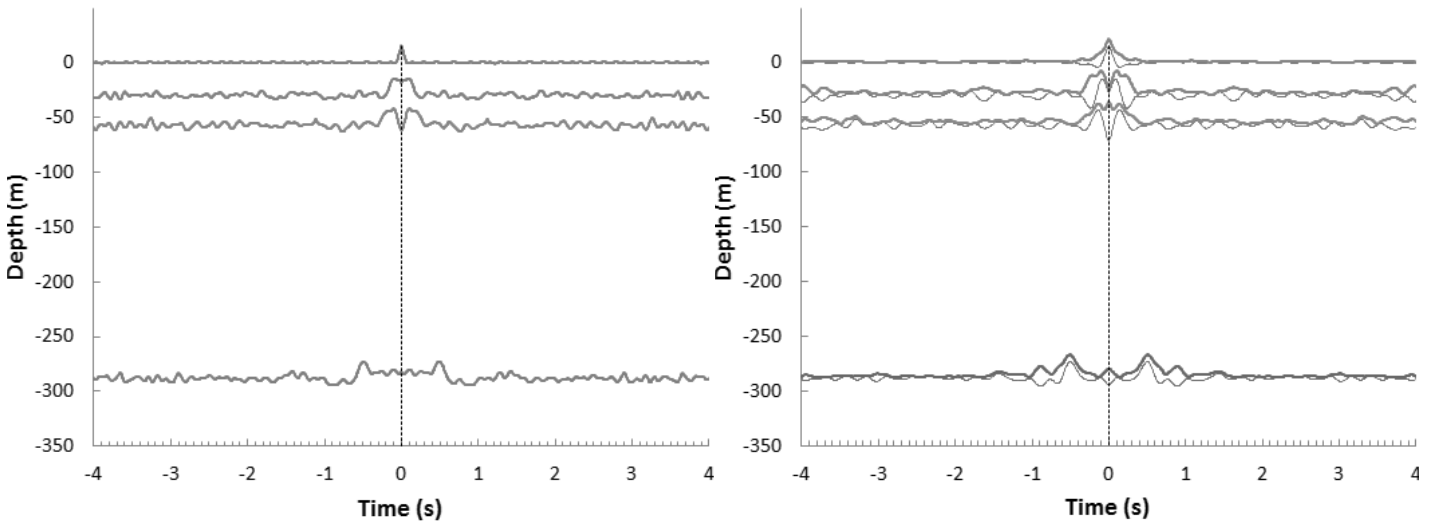


Fig. 14. Waveforms obtained by deconvolving the waves in the S-wave window of the NS component at each accelerometer depth with the waves in the S-wave window of the NS component at the surface a) deconvolution without filtering, and b) deconvolution after narrow band-pass filtering and envelope of the filtered and deconvolved waveforms

Next, the envelopes of the filtered and deconvolved waves are determined using the analytical signal defined as

$$E[d(t)] = d(t) + iH[d(t)] \quad (2)$$

where  $H[d(t)]$  represents Hilbert transform and  $i$  is the unit complex number. The envelope is obtained from the amplitude of the analytical signal (i.e.  $|E[d(t)]|$ ). In Figure 14b, envelopes of the deconvolved waves are also shown. Cross-correlation is then used to calculate travel times for the deconvolved waves and their envelopes. As expected, the travel times calculated from the envelopes are smaller than those calculated from the signal itself. It can be shown that the envelope functions are not affected by the dispersive properties of the medium (Bendat and Piersol, 1985). This property of envelope functions allows for determination of phase shifts which can be related to intrinsic attenuation through

$$\tau' \approx (1 - i(1/2Q))\tau \quad (3)$$

where  $\tau$  and  $\tau'$  are the travel times calculated from the filtered and deconvolved signal and its envelope, respectively and  $Q$  is the quality factor that represents intrinsic attenuation. The approximation given in (4) comes from the use of the complex wave velocity  $v_s + i\omega$  to in order to incorporate damping to wave propagation. By using the relationships  $1/Q = 2\omega/v_s$  and  $\tau' = h/(v_s + i\omega)$  where  $h$  denotes the thickness of layer, one can obtain

$$\tau' = (2Q/(2Q + i))\tau \quad (4)$$

Equation (4) can be approximated by Eq.(3) since  $Q \gg 1$  (Safak, 1995). Calculated average shear wave propagation velocities,  $Q$  factors and corresponding damping ratios for the soil layers between the accelerometers at ZYT site are presented in Table 2. Average  $V_s$  values inferred from PS-Logging tests are also given. An important advantage of the technique described above is that it provides a way to separate intrinsic attenuation and radiation damping.

Table 2. Dynamic properties of soil layers extracted from downhole records

Sensor Depth (m)	Thickness (m)	$V_s$ measured (m/s)	$V_s$ from deconvolved waveforms (m/s)	$V_s$ from envelope of deconvolved waveforms (m/s)	$Q$	Damping Ratio (%)
0	30	268	287	295	18	2.71
30	27	272	298	302	38	1.32
57	231	478	610	612	153	0.33
288	-	-	-	-	-	-

## CONCLUSIONS

Three geotechnical downhole arrays that are recently installed in the European Side of Istanbul is expected to provide valuable data for site response modeling given the existing high seismic activity of the region. Data recorded so far at ATK and ZYT downhole arrays represent low amplitude motions which allows for linear analysis of the soil response at these sites. Preliminary analysis of the data provides evidence for significant amplification of ground motion by the surface layers. More records of varying intensities would enable better understanding of soil response at these sites, particularly the shallow 'limestone' layer that is present at both sites. Data from downhole arrays also provide reference bedrock motion for the strong motion network that is in operation at the European side of Istanbul. Investigation of ground motions recorded at a total of 39 stations located at sites with comparable  $V_{s30}$  values demonstrates that  $V_{s30}$  alone is not a sufficient indicator of site amplification potential. In the meantime, application of a seismic interferometry technique to downhole records demonstrated that this approach can be used to extract dynamic properties of soil layers. Results of the study at ZYT site indicate using this approach, it is possible to calculate wave velocities and obtain in-situ intrinsic attenuation values. The approach will be further investigated to provide a practical way to monitor changes in the soil properties as the level of excitation increases.

## ACKNOWLEDGMENTS

Financial support for installation of downhole arrays are granted by TÜBİTAK, Istanbul Metropolitan Municipality, GFZ Potsdam and Boğaziçi University. The authors would like to acknowledge Prof. Mustafa Erdik, the coordinator of Istanbul Rapid Response Network, and Prof. Stefano Parolai, co-investigator at Megacity Istanbul Project. Barbaros Cetiner and Ahmet Korkmaz, members of project team for installing downhole arrays, are acknowledged for their tedious work in the field. The support of local municipalities of Bakırköy and Zeytinburnu as well as the personnel at Yunus Emre Cultural Center and Fatih Mosque is greatly appreciated.

## REFERENCES

- Ansal, A., A. Kurtuluş, and G. Tönük [2010], “Seismic Microzonation and Earthquake Damage Scenarios for Urban Areas”, *Soil Dyn. Earthquake Eng.*, Vol. 30, pp. 1319–1328.
- Bendat, J.S. and A.G. Piersol [1985], “*Random Data: Analysis and Measurement Procedures*”. John Wiley& Sons, New York.
- Beresnev, I. A., E.H. Field, P.A. Johnson, and den KE-A. Abeele [1998], “Magnitude of Nonlinear Sediment Response in Los Angeles Basin during the 1994 Northridge, California, Earthquake”, *Bull. Seism. Soc. Am.*, Vol. 88, pp. 1079-1084.
- Elgamal, A. W., M. Zeghal, H.T. Tang, and J.C. Stepp, [1995], “Lotung Downhole Array, I: Evaluation of Site Dynamic Properties”, *Jour. Geotech. Engrg., ASCE*, Vol. 121, No. 4, pp. 350–362.
- Erdik, M., Y. Fahjan, O. Özel, H. Alcik, A. Mert, and M. Gül [2003], “Istanbul Earthquake Rapid Response and the Early Warning System”, *Bull. Earthquake Eng.*, Vol. 1, pp. 157-163.
- Fukushima Y., K. Irikura, T. Uateke, and H. Matsumoto [2000], “Characteristics of Observed Peak Amplitude for Strong Ground Motion from the 1995 Kobe Earthquake”, *Bull. Seism. Soc. Am.*, Vol. 90, pp. 545-565.
- Idriss, I. M., and JI. Sun [1992], “*Shake91*”, A computer program for conducting equivalent linear seismic response analysis of horizontally layered soil deposits, modified based on the original SHAKE program by Schnabel, Lysmer and Seed, 1972.
- Kurtuluş, A., E. Şafak, A. Strollo, S. Parolai, and A. Ansal [2008], “Sensor Azimuth Determination at a Seismic Vertical Array in Istanbul, Turkey”, *European Seismological Commission ESC 2008, 31st General Assembly, Crete, Greece*.
- Mehta, K., R. Snieder, and V. Graizer [2007], “Downhole Receiver Function: a Case Study”, *Bull. Seism. Soc. Am.*, Vol. 97, No. 5, pp. 1396-1403.
- NEHRP (National Earthquake Hazards Reduction Program) [2001], “*Recommended Provisions for Seismic Regulations for New Buildings and Other Structures*”, 2000 Edition, Part 1: Provisions (FEMA 368), Ch. 4, Washington, D.C.
- OYO [2007], “Production of Microzonation Report and Maps –on European Side (south)”, Final Report to Istanbul Metropolitan Municipality.
- Şafak, E. [1995], “Discrete-time Analysis of Seismic Site Amplification”, *Jour. Engrg. Mechanics, ASCE*, Vol.121, No.7, pp.801-809.
- Snieder, R., and E. Şafak [2006], “Extracting the Building Response using Seismic Interferometry; Theory and Application to the Millikan Library in Pasadena, California”, *Bull. Seism. Soc. Am.*, Vol. 96, No. 2, pp. 586-598.
- Trifunac, M. D, and M. I. Todorovska [1998], “Nonlinear Soil Response as a Natural Passive Isolation Mechanism- the 1994 Northridge, California, Earthquake”, *Soil. Dyn. Earthquake Eng.* (17): 41-51.